New applications for known drugs: Human glycogen synthase kinase 3 inhibitors as modulators of Aspergillus fumigatus growth

Víctor Sebastián-Pérez, Maria-Tsampika Manoli , Daniel I Pérez, Carmen Gil, Emilia Mellado, Ana Martínez, Eduardo A Espeso, Nuria E Campillo.

Eur J Med Chem. 2016 Jun 30;116:281-289.

https://doi.org/10.1016/j.ejmech.2016.03.035

New applications for known drugs: Human Glycogen Synthase Kinase 3 inhibitors as modulators of *Aspergillus fumigatus* growth

Víctor Sebastián[a], Maria-Tsampika Manoli[a], Daniel I. Pérez[a], Carmen Gil[a], Emilia Mellado[b], Ana Martínez[a], Eduardo A. Espeso[a], Nuria E. Campillo*[a].

[a]Centro de Investigaciones Biológicas (CIB, CSIC). Ramiro de Maeztu, 9, 28040-Madrid, Spain.

[b]Centro Nacional de Microbiología, Instituto de Salud Carlos III, 28220-Madrid, Spain.

AUTHOR INFORMATION

*Corresponding Author

Tel.: +34 91 837 31 12;Fax: +34 91 536 04 32; e-mail: nuria.campillo@csic.es

Abstract

Invasive aspergillosis (IA) is one of the most severe forms of fungi infection. IA disease is mainly due to *Aspergillus fumigatus*, an air-borne opportunistic pathogen. Mortality rate caused by IA is still very high (50-95%), because of difficulty in early diagnostics and reduced antifungal treatment options, thus new and efficient drugs are necessary. The aim of this work is, using *A. nidulans* as non-pathogen model, to develop efficient drugs to treat IA.

The recent discovered role of glycogen synthase kinase-3 homologue, GskA, in *A. fumigatus* human infection and our previous experience on human GSK-3 inhibitors focus our attention on this kinase as a target for the development of antifungal drugs.

With the aim to identify effective inhibitors of colonial growth of *A. fumigatus* we use *A. nidulans* as an accurate model for *in vivo* and *in silico* studies. Several well-known human GSK-3β inhibitors were tested for inhibition of *A. nidulans* colony growth. Computational tools as docking studies and binding site prediction was used to explain the different biological profile of the tested inhibitors. Three of the five tested hGSK3β inhibitors are able to reduce completely the colonial growth by covalent bind to the enzyme. Therefore these compounds may be useful in different applications to eradicate IA.

Keywords: *Aspergillus nidulans*, *Aspergillus fumigatus*, docking, Fpocket, GSK-3 inhibitors

Graphical Abstract:

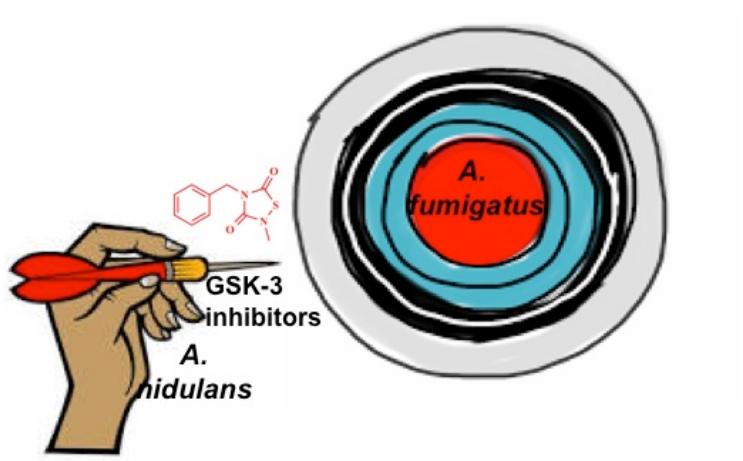

1. Introduction

In ascomycetes, *Aspergillus spp.* are among the most common filamentous fungi found in nature, being their impact on humans from beneficial to harmful [1]. Some of the *Aspergillus* species are of industrial and medical significance. For instance, *A. oryzae* and *A. niger* are widely used in industry for synthesis of enzymes and aditives, and food production such as proteases, citric acid, miso, sake or soy sauce. In contrast, *A. flavus* produce one of the most potent mycotoxins, the carcinogen aflatoxins, which contaminate various plant- and animal-based foods. Importantly, *A. fumigatus* [2, 3] is an ubiquitous and saprophytic organism considered by many pathologists to be the world's most harmful mold. It is a life-threatening human pathogen that causes 90% of invasive aspergillosis (IA) becoming the most prevalent airborne fungal pathogen in developed countries. Invasive aspergillosis in immunocompromised patients results in a high mortality rate, up to more than 50% of cases. Prophylaxis, early diagnosis and early initiation of antifungal therapy are of utmost importance for the reduction of IA related mortality [4]. However, and despite all advances in the management of IA, important questions remain unresolved and the search for specific therapeutic agents is a social need [5].

A. nidulans, *Emericella nidulans* in its teleomorph state, is a saprophyte able to utilize a wide range of nutritional sources and to tolerate diverse physico-chemical conditions as extreme pH values or elevated concentrations of cations. Due to these facts and the easy handling in the laboratory, *A. nidulans* has historically been a robust model system for the discovery of genes involved in fungal specific processes such as primary and secondary metabolite production (i.e. penicillin biosynthesis), or universal key elements and regulators of the cell cycle (i.e gamma tubulin). Also, because of being closely related to the rest of *Aspergillus* species it has been used as one of the critical fungal systems in genetics and cell biology [6], and it may be used as pharmacological tool for the search of novel antifungal drugs [7].

Another major contribution of ascomycetes has been to the understanding of adaptation to ambient pH and saline stress, and of calcium signaling. In *A. nidulans* two novel pathways have been discovered in relationship with tolerance to alkalinity and cation stress, those mediated by the zinc finger transcription factors *PacC* and *SltA* [8, 9] (see also Fig. 1a for Slt pathway). Of

great interest for development of antifungal drugs is the existence of fungal specific pathways and the *Slt* pathway is exclusively distributed among pezizomycotina, representing most of filamentous fungi of commercial and clinical interest [10].

The calcium induced calcineurin mediated pathway is widely presented in eukaryotes, from fungi to humans. Although final effectors are different, for example calcineurin-responsive-zinc fingers (CRZs) in fungi (yeast and filamentous) and nuclear factors for activated T-cells (NFATs) in mammals [11-13], the signaling cascade follows a highly conserved structure and functional elements are easily identified (Fig. 1a). One of these signaling elements is the glycogen synthase kinase (Gsk) and its homologues.

Human glycogen synthase kinase 3 (GSK-3), with two isoforms α and β, is a serine/threonine kinase with a wide spectrum of targets, including transcription factors, regulators of apoptosis and cell differentiation [14]. During the last year the relevance of GSK-3 homologues in *Aspergillus spp* has been evidenced. By one hand the homologue of the human GSK-3β in *A. nidulans*, namely GskA, was identified and, although not being essential for the fungus, its absence severely debilitates colonial growth [12, 15]. For example, a conditional expression of the *gskA* gene driven by the ethanol inducible alcohol dehydrogenase I promoter, $alcA^{p}$, reveals the important role of GskA in colony morphology and development (Fig. 1b). In the recombinant strain, repression of the *alcA* promoter leads to absence of GskA protein and strong reduction in colony diameter (Figs. 1c, d) [12, 15].

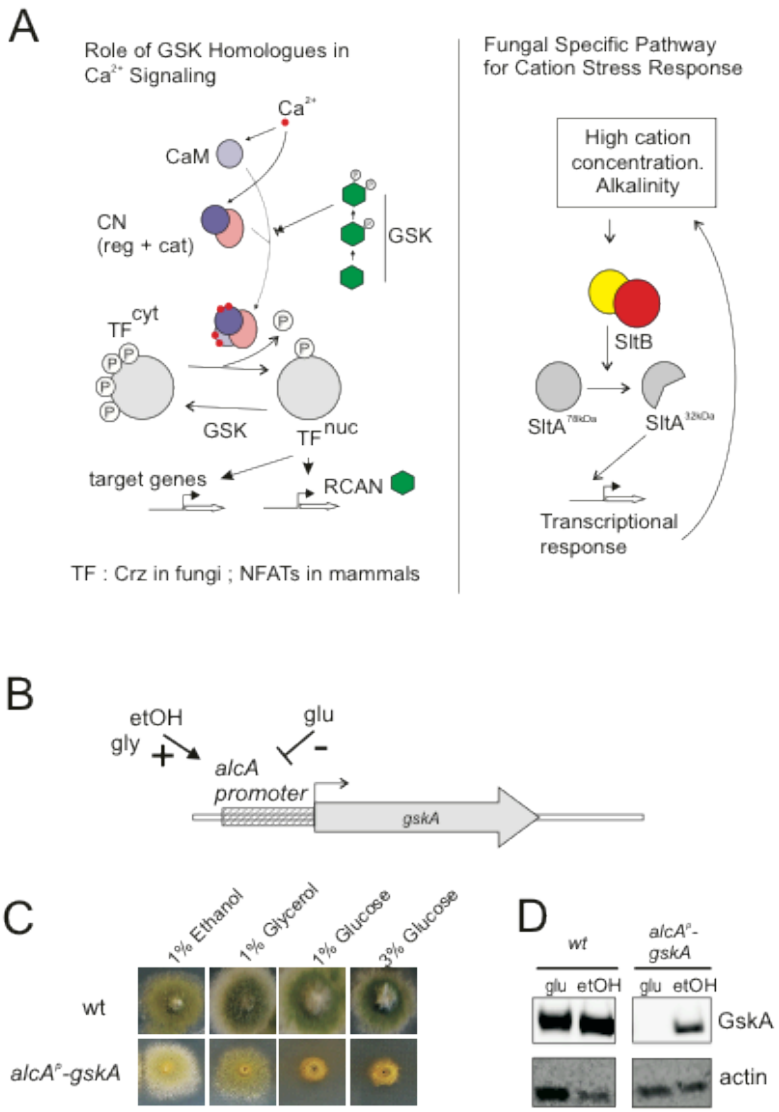

Fig. 1. Important role of GskA, the orthologue of GSK-3β, in fungal colony growth. a) In *Aspergilli,* GSK homologues participate in the calcium (Ca^{2+}) calcineurin signaling pathway as in higher eukaryotes. Components are identifiable among species, CaM (calmodulin), catalytic and regulatory subunits of calcieurin (RCAN). GskA will act at two levels, phosphorylating RCAN and the TF (Crz in fungi, NFAT in metazoans). Solely in filamentous fungi, the Slt pathway mediates the response to high extracellular concentrations of cations and alkalinity. The SltB protein signals the TF SltA to generate its active form. b) The *gskA* gene of *A. nidulans*, coding for GskA kinase, was conditionally regulated by the ethanol inducible promoter *alcA* and colonial growth was

evaluated. A schematic representation of the regulatory mechanisms mediating the transcriptonal regulation of the alcohol dehydrogenase I promoter *alcA*. The presence of glucose (glu) represses *alcA* promoter but ethanol (EtOH) or glycerol (gly) activates its expression. c) A wild-type strain (MAD5515) shows normal colonial morphology on AMM containing the indicated concentrations of carbon sources. The strain carrying the $alcA^{p}$-driven *gskA*, showed a strong reduction in colonial growth when the expression of alcA promoter was inhibited by glucose. d) GskA levels detected in protein extracts from mycelia of strains MAD5515, expressing GskA-GFP fusion driven by the *gskA* endogenous promoter, and MAD5544, expressing GskA-GFP driven by the *alcA* promoter, cultured in repressing (glu) or activated (etOH) conditions for *alcA* promoter. GskA-GFP fusion was visualized in WBs using an anti-GFP antibody. Detection of actin was used as loading control.

Thus, based on the elevated sequence identity (nearly 92%) of Gsk homologues from *A. fumigatus* and *A. nidulans* [16], the advantages of the latter as genetic and biology model together with our experience in the development of human GSK-3β inhibitors [17-20], we proposed the development of effective inhibitors of colonial growth of *A. fumigatus* by using *A. nidulans* as an accurate model for both *in silico* and *in vivo* studies. To reach this goal, we have employed different *A. nidulans* strains and several computational techniques in order to perform homology modelling studies, druggable pocket detection and docking studies.

2. Results and discussion

2.1. *In vivo studies*

To find potential drugs against *Aspergilli*, several well-known human GSK-3β inhibitors [17-20] were tested phenotypically for inhibition of *A. nidulans* colony growth. Chemical structures of these inhibitors together with the IC_{50} value on human GSK-3β and their binding mode to the enzyme are depicted in figure 2.

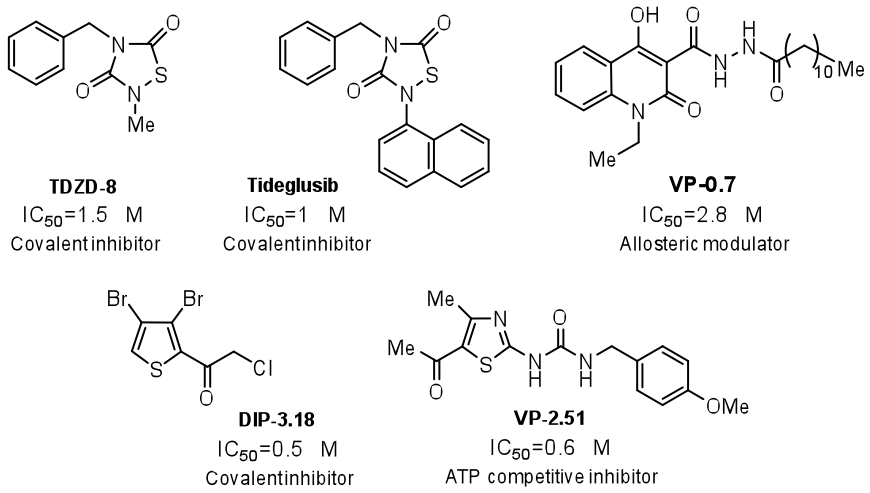

Fig. 2. Chemical structures of human GSK-3β inhibitors tested together with values of their IC_{50} values and binding mode to GSK-3β

To prevent crossed effects due to auxotrophic mutations, common in strains of the fungal model, we used in this study prototrophs able to grow on synthetic minimal medium (AMM) supplemented only with nitrogen and carbon sources. AMM was used to score the effect of these GSK-3β inhibitors on the colonial growth of *Aspergilli*. A prototroph wild-type strain of *A. nidulans* (MAD4096) tolerated elevated concentrations of **VP-07** and **VP-2.51** (Fig. 3). Complete growth inhibition was detected with **TDZD-8** at 50 μM (Fig. 3). Interestingly, **tideglusib**, a closely related structural compound to **TDZD-8** in clinical trials for several neurological disorders, did not cause a such significative reduction in colonial growth of MAD4096 strain. Since GskA is involved in the calcineurin-mediated signaling of CrzA the effect of these inhibitors was also tested with the null *crzA* strain (*crzA*Δ, MAD4100). The *crzA* null mutant strain displayed the same tolerance to the set of inhibitors tested as the wild-type strain. However, the mutant *sltA*Δ strain (MAD4097) displayed a strong sensitivity to **DIP-3.18** as observed for the wild type, but a stronger effect of **TDZD-8** and **tideglusib**. Colonial diameter of *sltA*Δ strain was reduced to 50% using 10 μM of **TDZD-8** and impaired growth was observed with 50 μM of **tideglusib**.

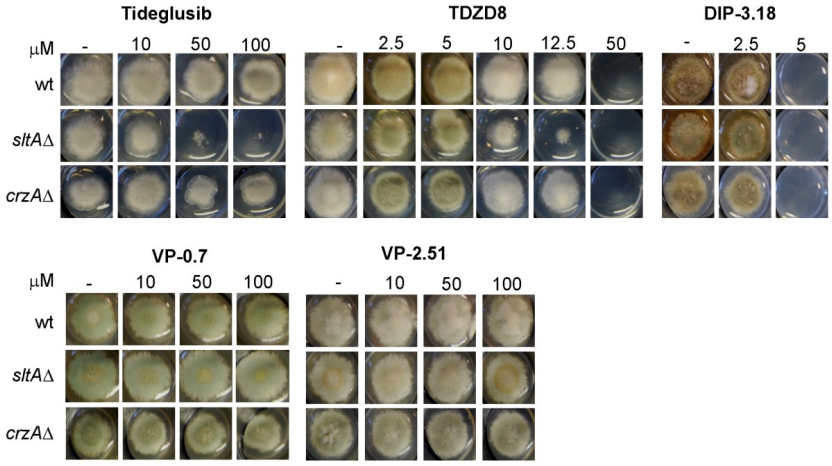

Fig. 3. Sensitivity of *A. nidulans* to inhibitors of human GSK-3β Three prototroph *A. nidulans* strains were analyzed for their tolerance to increasing concentrations of a range of known *in vitro* inhibitors of the GSK-3β kinase. Conidial suspensions were point inoculated onto AMM containing the indicated concentration of inhibitor (name of inhibitor and concentration at the top of each inset). Colonial growth was evaluated after 72 h post inoculation and incubation at 37ºC. wt indicates the wild-type prototroph strain MAD4096, and below are the prototroph mutants for transcription factors SltA (*sltA*Δ, strain MAD4097) and CrzA (*crzA*Δ, strain MAD4100).

Thus, analyzing the results we can conclude that **VP-2.51** and **VP-0.7** do not affect to the colonial growth, meanwhile **tideglusib**, **TDZD-8** and **DIP-3.18** are able to reduce severely fungi viability.

In order to explain these biological differences, we decided to explore the mode of binding of these inhibitors in *A. nidulans* GskA using computational techniques.

2.2. Computational study

Drug-like characterization. QikProp predicts physically significant descriptors and pharmaceutically relevant properties of organic molecules. Analyzing in detail these physico-chemical properties of the selected compounds, we found that in general the compounds studied are drug-like molecules. However, several differences for **VP2.51** comparing to the rest of the compounds have been found such as predicted Caco-2 cell permeability or metabolic stability (Table 1). These differences may indicate that this compound is poorly

absorbed by the fungus system and can also suffer metabolic reactions before achieving its target. The rest of compounds present excellent drug-like properties, a great predicted Caco permeability, and just one potential predicted metabolic reaction.

Table 1. Physico-chemical properties of GSK-3β inhibitors

Nuria Campillo 29/2/16 13:26
Con formato: Fuente:Negrita

Structure	QPPCaco	#metab
TDZD-8	1733.441	1
VP-2.51	312.998	4
Tideglusib	2189.918	1
DIP3-18	3696.31	2

Homology modeling. The absence of the three-dimensional structure for GskA prompted us to construct its homology model in order to perform of docking studies and potential binding sites in GskA.

All *Aspergillus* Gsk sequences have a high identity level with human GSK3β as showing in figure S1. Sequentially, the ascomycete *A. nidulans* GskA shares 62.8% of identity with human GSK-3β, while this identity reaches 72% when comparing with UmGSK3, the GSK-3β homologue from the basidiomycete plant-pathogen *Ustilago maydis* (UmGSK-3) [21]. The sequential alignment of theses sequences is shown in figure 4.

```
A.nidulans        --------------MSQNRSGVFSNLRMG------------------EVV 18
A.fumigatus       --------------MSQNRPGVFSNLRMGENITQEPVELTALLSDHTEVV 36
U.maydis          -------------GSFTMSNAPLNGVKLN------------PLDDPNKVI 25
Human             MSGRPRTTSFAESCKPVQQPSAFGSMKVS------------RDKDGSKVT 38
                                  . :..:::.                 :*

A.nidulans        REKVQDGL-TGETKEIQYSQCKIVGNGSFGVVFQTKMMPSGEDAAIKRVL 67
A.fumigatus       REKVQDGL-TGETKEISYSQCKIVGNGSFGVVFQTKMMPSGEDAAIKRVL 85
U.maydis          KVLASDGK-TGEQREIAYTNCKVIGNGSFGVVFQAKLVESDE-VAIKKVL 73
Human             TVVATPGQGPDRPQEVSYTDTKVIGNGSFGVVYQAKLCDSGELVAIKKVL 88
                     .  *  ... :*: *:: *::********:*:*:  *.* .***:**

A.nidulans       QDKRFKNRELQIMRIVRHPNIVELKAFYYSNGERKDEVYLNLVLEYVPET 117
A.fumigatus      QDKRFKNRELQIMRIVRHPNIVELKAFYYSNGERKDEVYLNLVLEYVPET 135
U.maydis         QDKRFKNRELQIMRIVKHPNVVDLKAFFYSNGDKKDEVFLNLVLEYVPET 123
Human            QDKRFKNRELQIMRKLDHCNIVRLRYFFYSSGEKKDEVYLNLVLDYVPET 138
                 ************** : * *:* *: *:**.*::****:*****:*****

A.nidulans       VYRASRYFNKLKTTMPMLEVKLYIYQLFRSLAYIHSQGICHRDIKPQNLL 167
A.fumigatus      VYRASRYFNKLKTTMPMLEVKLYIYQLFRSLAYIHSQGICHRDIKPQNLL 185
U.maydis         VYRASRHYAKLKQTMPMLLIKLYMYQLLRSLAYIHSIGICHRDIKPQNLL 173
Human            VYRVARHYSRAKQTLPVIYVKLYMYQLFRSLAYIHSFGICHRDIKPQNLL 188
                 ***.:*:: : * *:*:: :***:***:******** *************

A.nidulans       LDPATGILKLCDFGSAKILVENEPNVSYICSRYYRAPELIFGATNYTTKI 217
A.fumigatus      LDPSTGILKLCDFGSAKILVENEPNVSYICSRYYRAPELIFGATNYTTKI 235
U.maydis         LDPPSGVLKLIDFGSAKILIAGEPNVSYICSRYYRAPELIFGATNYTTNI 223
Human            LDPDTAVLKLCDFGSAKQLVRGEPNVSYICSRYYRAPELIFGATDYTSSI 238
                 *** :.:*** ****** *: .**********************:**:.*

A.nidulans       DVWSTGCVMAELMLGQPLFPGESGIDQLVEIIKVLGTPTREQIRTMNPNY 267
```

```
A.fumigatus      DVWSTGCVMAELMLGQPLFPGESGIDQLVEIIKVLGTPTREQIRTMNPNY 285
U.maydis         DIWSTGCVMAELMQGQPLFPGESGIDQLVEIIKVLGTPSREQIKTMNPNY 273
Human            DVWSAGCVLAELLLGQPIFPGDSGVDQLVEIIKVLGTPTREQIREMNPNY 288
                 *:**:***:***: ***:***:**:*************:****: *****

A.nidulans       MEHKFPQIKPHPFNK-------------VFR-KAPHEAIDLISALLEYTP 303
A.fumigatus      MEHKFPQIKPHPFNK-------------VFR-RAPHEAIDLISALLEYTP 321
U.maydis         MEHKFPQIRPHPFSK-------------VFRPRTPPDAIDLISRLLEYTP 310
Human            TEFKFPQIKAHPWTKDSSGTGHFTSGVRVFRPRTPPEAIALCSRLLEYTP 338
                  *.*****:.**:.*             *** ::* :** * * ******

A.nidulans       TQRLSAIEAMCHPFFDELRDPNTKLPDSRHPNGAARDLPNLFDFSRHELS 353
A.fumigatus      TQRLSAIEAMCHPFFDELRDPNTRLPDSRHPGGAARDLPNLFDFSRHELS 371
U.maydis         SARLTAIEALCHPFFDELRTGEARMPN-------GRELPPLFNWTKEELS 353
Human            TARLTPLEACAHSFFDELRDPNVKLPN-------GRDTPALFNFTTQELS 381
                 : **:.:** .*.******  :.::*:       .*: * **::: .***

A.nidulans       IAPSMNSRLVPPHSRPALEARG---------LYIDDFKPLKKEEMMAHLD 394
A.fumigatus      IAPALNSRLVPPHARAALEARG---------LDIDNFTPLTKEEMMARLD 412
U.maydis         VRPDLISRLVPQHAEAELLSRG---------IDVHNFQPIPLESLKVTLD 394
Human            SNPPLATILIPPHARIQAAASTPTNATAASDANTGDRGQTNNAASASASN 431
                   * : : *:* *:.    :              :            :
```

Fig. 4. Sequence alignment of human GSK-3β (P49841-2), and fungal homologues *A. nidulans* (Q5AYX2), *A. fumigatus* (Q4WDL1) and *U. maydis* (PDB: 4E7W).

A further analysis of the alignment allowed us to identify a significant change in a residue of the catalytic site in *Ustilago maydis* sequence. This mutation (Cys by Ile) affects to a key residue involved in the ligand binding. As it has been previously reported, the inactivation of the human enzyme by **TDZD-8** and **tideglusib** ligands is due to the formation of a covalent sulfur-sulfur bond between this key cysteine located at the entrance of the ATP site of human GSK-3β [22]. Consequently, because of the absence of this cysteine residue in the *Um* GSK-3 structure, it was dismissed as template to build the model.

Two models were constructed using SWISS-MODEL with different templates (two human GSK-3β structures 1I09 [23] and 1Q5K [24]) (Table S2).

The predicted models were checked for *psi* and *phi* torsion angles using the Ramachandran plot (Fig. S2). The results show that favorable combinations of *phi-psi* values in the residues reach 95% for the model using 1Q5K, human GSK-3β as template. The rate of outlier residues reaches 1.5% for 1Q5K model while in the other model is more than 2%, therefore according to *phi-psi* values it is an accurate model to carry out further studies. The RMSD (root mean square deviation), QMEAN [25] and Verify 3D [26] are gathered in the table S2. According to all this data, model based on 1Q5K was chosen for docking studies in order to obtain the most reliable results.

Cavities prediction on GskA surface. Detection, comparison and analyses of ligand binding pockets are pivotal to structure based drug design endeavors.

Mainly there are two types of algorithms used to this end, evolutionary and structure based algorithms. Here, free geometry-based algorithm Fpocket [27] has been used to identify pocket binding sites in the *A. nidulans* GskA model and comparing them to the validated human GSK-3β druggable pockets [17].

Carefully inspection of the results allowed pinpointing several facts. We are able to recognize most of the highly reproducible cavities described for human GSK-3β in the *A. nidulans* GskA model (Fig. 5). Moreover, most of the key residues in the catalytic site and in other allosteric binding sites are conserved. All the data regarding the volume and score of different pockets is shown in Table S3 (see supplementary material), as well as the presence of the significant residues in every pocket.

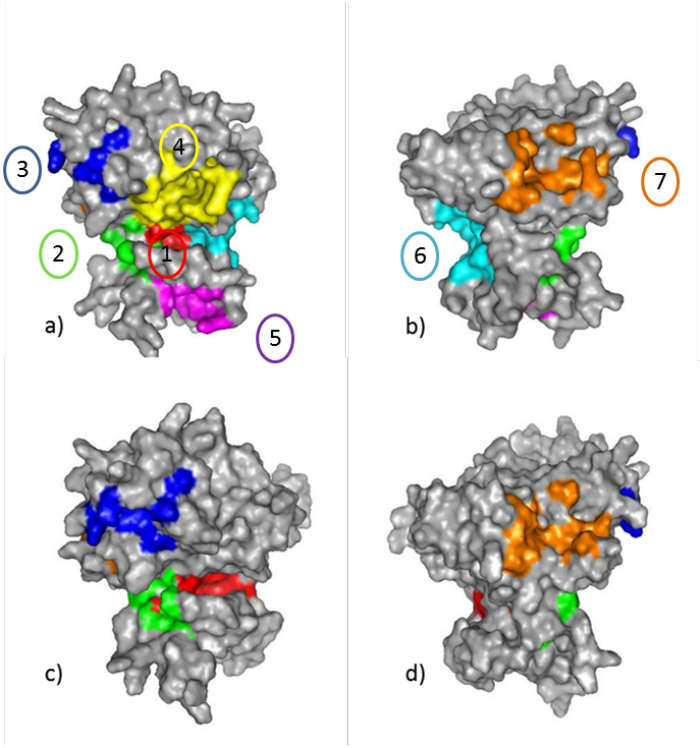

Fig. 5. a) b) Most relevant known pockets for human GSK-3β, numbered according to former cavity studies. c) d) Homologous pockets found in the cavity detection studies for GskA in *A. nidulans.* Pockets are colored regarding human GSK-3β pockets.

The comparative data regarding most important and conserved human pockets *vs A. nidulans* GskA found cavities with all the residues is shown in figure S4. The numbering of human GSK-3β pocket has been carried out according to former cavity studies in this protein [17].

It is remarkable the change of the conserved arginine (R209) in the human GSK-3β by a glutamic acid in the GskA model. It has been reported the fact that this arginine is a key residue in the binding pocket for some ligands, such as the allosteric inhibitor **VP-0.7** [17]. In GskA, differences in charge and volume in this pocket may well affect the interaction with some ligands, as might be the case for **VP-0.7.** According to the Fpocket analysis, the drastically change in terms of volume and charge in the binding pocket #7 (GSK-3β numbering) due to the replacement of the highly conserved arginine in human GSK-3β by the glutamic acid in GskA may explain the biological result. Therefore, both the size and the residue change in pocket #7 can explain why **VP-0.7** is not an inhibitor of GskA.

Docking studies. In order to explain their biological profile, autodock docking studies of the all compounds **(tideglusib**, **TDZD-8**, **DIP-3.18** and **VP-2.51**) were performed

Blind docking. It is an approach very useful to search the entire surface of proteins for binding sites while simultaneously optimizing the conformations of the ligands. Thus, we performed a blind docking with two representative ligands such as **VP-2.51** and **tideglusib**. Results shown that binding site of **tideglusib** is similar than the published binding site in human GSK3β [22]. Tideglusib binds to GskA in the same pocket of human GSK3β very close to Cys 178 (GskA numbering), pointing out a possible formation of covalent bond as in human GSKβ. However, **VP-2.51** presents an alternative binding site compared to human GSK3β (Figure 6), Thus the inhibition is not as covalent binding mechanism as the rest of compounds. This fact allows us to explain the different *Aspergillus spp. in vivo* activity of this compound compared to the rest of human GSK-3β inhibitors.

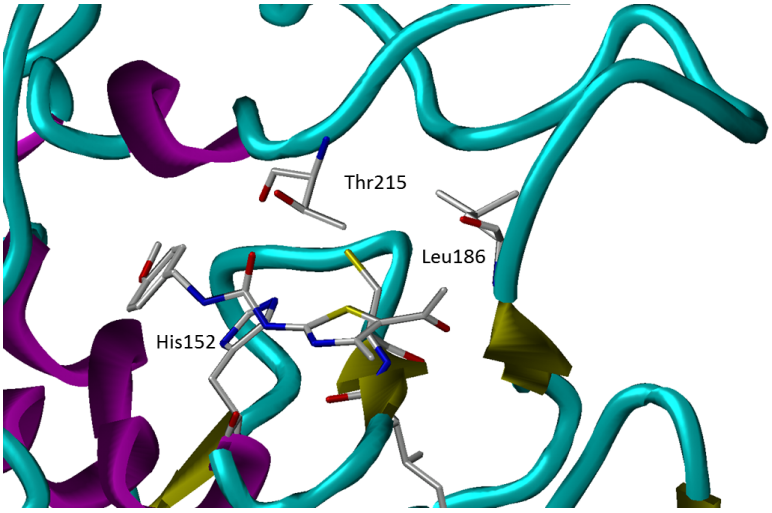

Figure 6. Docking solution of VP-2.51

Focus docking. Two approaches were used for **tideglusib**, **TDZD-8** and **DIP-3.18** ligands. The first one is a regular docking (see Fig. S4) and the second one is a covalent docking. This covalent docking was performed taking into account that the three ligands bind the catalytic site (Fig. 7) of the GSK-3β by a covalent bond between the cysteine of the pocket and the sulfur present in the ring of both ligands [22].

In general, regular docking for the three compounds showed similar results. Table 2 gathers the distance of S-S bond to the best clusters of each compound. Regarding **tideglusib**, the 85% of the resulting conformations were classified in the three best-scored clusters found meanwhile to **TDZD-8** almost 90% of conformations were classified in the best two clusters and to **DIP-3.18** two main clusters have 80% of the total conformations generated by the program.

Table 2. Distance (Å) of S-S bond in the best-scored cluster (most populated, better energy) of **tideglusib**, **TDZD-8** and **DIP-3.18**

Cluster	**Tideglusib**	**TDZD-8**	**DIP-3.18**
1	3.2-6.6	5.5-6.7	4.7-5.7
2	3.7-7.2	3.5-4.5	4.4-5.5
3	3.2-4.4	-	-

As shown in table 2, the distances corresponding to the covalent bond are greater for this type of bond. Although these distances are analogous to the ones calculated in the docking results for GSK-3β in which exists a covalent bond [22].

For the second approach, a covalent docking was performed for the compounds. In the case of **tideglusib**, a vast majority cluster was found with more than 95% of the conformations and distances in the range of 1.6-2.0 Å. For the **TDZD-8**, over 85% conformations were found in the same cluster and distances were between 1.8-2.0 Å, and for **DIP-3.18** is 1.7 Å. Best-scored conformations in covalent dockings for both compounds are shown in figure 6.

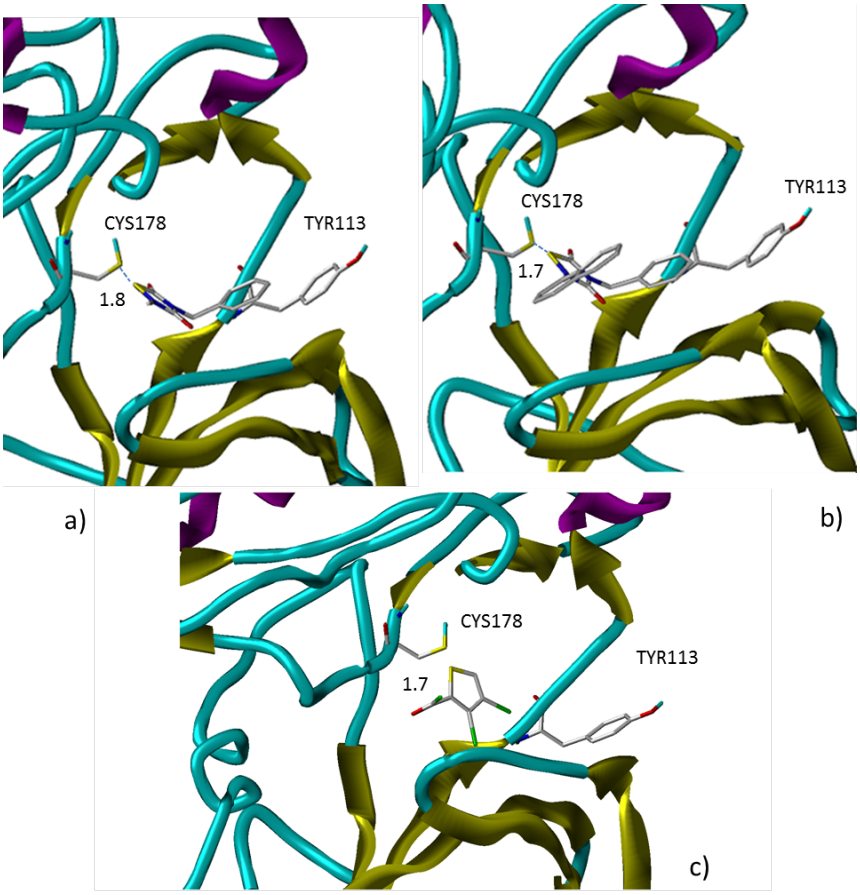

Fig. 7. Covalent docking solutions for a) **tideglusib**, b) **TDZD-8** and c) **DIP-3.18.** The distances are in Å

As docking positions and interactions sites are quite similar among these compounds (Fig. S5a) we show here the complete results for one of them, **TDZD-8**.

Interactions ligand-protein were also studied for the best binding energy conformation of every cluster, regarding both approaches for **TDZD-8**, with the LPC program (Table S4). No hydrogen bonds were found but in **TDZD-8** regular covalent docking; all conformations interacts aromatically with Tyr 113 and most important hydrophobic interactions are Val 41, Val 49, Lys 64, Ala 62, Asp 179, Leu 111, as it is shown in Table S4 (Fig. S5b).

2.3. Sensitivity of *Aspergillus fumigatus*

Based on the tolerance tests done with the model *A. nidulans*, the effect of **tideglusib**, **TDZD-8** and **DIP-3.18** was analysed in the pathogen *A. fumigatus* (Fig. 8). In AMM similar dilution series of these GSK-3β inhibitors were analysed for three prototroph wild-type strains of *A. fumigatus*: CM237, AF293 and CBS144. Essentially, tolerance results were comparable to those found with the model organism. Tolerance to 100 μM **tideglusib** and inhibition of colony growth with 50 μM **TDZD-8** for the three strains analysed and results were similar between 48 and 72 h of incubation. Interestingly the strain CBS144 displayed sensitivity to 5 μM **DIP-3.18** as observed with *A. nidulans*, but CM237 and AF293 were able to tolerate this concentration after 72 h incubation, although sensitivity was observed at 48 h. These results indicate that **TDZD-8** is probably an effective inhibitor of colonial growth in *Aspergilli* and tolerance to **DIP-3.18** may differ among strains and species.

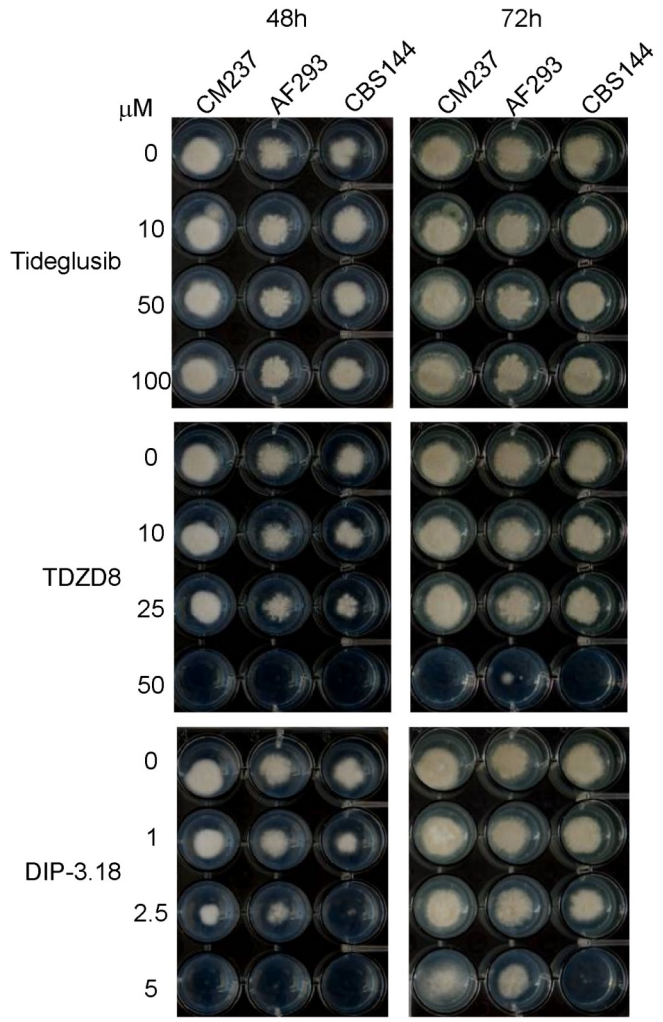

Fig. 8. Sensitivity of wild-type *A. fumigatus* strains CM237, AF293 and CBS144 to three inhibitors of GSK-3β kinase. Conidial suspensions were inoculated onto AMM medium containing the indicated concentration of inhibitors. Colonial growth was scored after 48 and 72 h of incubation at 37ºC.

3. Conclusions

Aspergillus fumigatus is currently the major airborne fungal human pathogen in developed countries. It is able to cause several forms of disease in humans of which invasive aspergillosis in immunocompromised patients is the most

severe. *A. fumig*atus has the ability to adapt to a wide range of environmental conditions living under extensive environmental stress, including air-conditioning pipes. The high mortality rate of this disease prompts us to look for new drugs against invasive aspergillosis and/or new antifungal agents that may be used as prophylactic disinfectants. The recent discovered role of GSK-3β [14] in *A. fumigatus* human infection and our previous experience on human GSK-3β inhibitors for neurological disorders focused our attention to this kinase as target for our antifungal drug discovery program. We have shown that using *A. nidulans* as a well-established screening pharmacological tool, we have identified several human GSK-3β inhibitors as potent inhibitors of *A. fumigatus*. The strong sequence similarity between human GSK-3β and GskA allows the study of structure activity relationships and provides new clues for future drug design and for selecting the better human kinase inhibitors to fight against invasive aspergillosis.

Three out of five most common human GSK-3β inhibitors are able to strongly reduce the colonial growth of *A. nidulans*, being their covalent binding to the fungal kinase the most likely mechanism of inhibition. Despite **VP-2.51** is theoretically able to bind GskA it is not effective in reducing the colonial growth, probably due to an alternative non-covalent mode of inhibition.

The discovery of some human GSK-3β inhibitors as potent agents against *A. fumigatus* has important translational consequences because with the same drug, the external infective agent will be killed and the immune response of the host will be improved. This synergy merits will be confirmed in future clinical trials of GSK-3β inhibitors for aspergillosis treatment.

4. Experimental section

4.1 Biological methods

Strains and media

A. nidulans strains used in the present study for testing the inhibitors of GSK were MAD4096 (wild type prototroph), MAD4097 (*sltA*Δ prototroph), MAD4100 (*crzA*Δ prototroph). Strain MAD1425 (*pyrG89,argB2;pyroA4,nkuA*Δ*::argB*)[28] was used as a recipient for the generation of strains expressing GFP tagged versions of GskA, driven by the *gskA* endogenous promoter, strain MAD5515 (*pyrG89,argB2;pyroA4,nkuA*Δ*::argB;gskA-gfp-pyrG*^{Af}), and by the *alcA*

promoter, strain MAD5544 (*pyrG89,pyroA*^{Af}*::alcA::gskA-GFP-pyrG*^{Af}*;argB2;pyroA4,nkuAΔ::argB*). Strains CM237, AF293, CBS144 are wild-type prototrophs of *A. fumigatus*. *A. nidulans* strains were cultivated in appropriately supplemented standard minimal medium (AMM) and complete medium (ACM) for propagation and obtaining conidiospores, as described previously [28]. For total protein extractions, strains were cultivated in fermentation media [12] supplemented with 1% Glucose or 1% Ethanol for 18h at 37ºC under agitation.

Construction of strains

Standard molecular biology techniques for the generation of transformation cassettes and plasmids were performed as previously described.[28] The transformation cassette for *gskA::gfp* construct was generated by fusion PCR procedures using oligonucleotides listed in Table S1. A detailed representation of the construction of recombinant *gskA* loci is shown in figure S7. Recombinant *A. nidulans* strains were obtained by transformation using linear DNA fragments or plasmids following the procedures described in reference [29]. Gene replacements were favored by the presence of null *nkuA* allele [30]. Transformants were selected on the basis of complementation of *pyrG89* or *pyroA4* mutations using homologues from *A.* fumigatus [28]. Pyrimidine or pyridoxine prototrophs were selected and homokaryotic transformants carrying single-copy integration events were identified by PCR or Southern blotting.

Protein extraction and analysis procedure

Mycelia were collected by vacuum filtered using 0.45 μm-pore-size nitrocellulose membranes (Scharlau) and frozen in dry ice. Frozen samples were lyophilized for 16h before protein extraction. In order to prevent protein degradation, the alkaline lysis extraction procedure was used [12].

For Western blotting proteins were resolved in 4-15% Mini PROTEAN® TGX ™ precast polyacrylamide gels (Biorad) and subsequently transferred to nitrocellulose filters using TransBlot®Turbo™ Transfer System (Biorad). GFP tagged proteins were detected using mouse anti-GFP (1/5000; Roche). Actin, detected with mouse anti-γ-actin antibody (1/50000; ICN Biomedicals), was used as loading control. Peroxidase activity was detected with Amersam Biosciences ECL kit.

Inhibitor assays

Growth of *A. nidulans* and *A. fumigatus* was evaluated on AMM containing different concentrations of inhibitors. The inhibitors used in these assays were dissolved in DMSO, usually a stock solution was prepared at a fixed concentration of 50 mM. Growth tests were performed in 24-multiwell plates containing 1 ml of AMM plus inhibitor. To avoid a cross effect of DMSO, 10 μl of each inhibitor solution was added to the melted AMM medium. As control, the same amount of DMSO was added to AMM. 10^3 spores of *Aspergillus*, calculated using a Neubauer chamber, were centrally inoculated on each well. The plates were incubated at 37ºC for 72h and then photographed.

4.2 Computational methods

Ligand characterization

Tideglusib, TDZD-8 and VP2.51 were selected to be further analyzed taking into account their physico-chemical properties. The preparation of the compounds and the 2D-to-3D conversion was performed using LigPrep tool, a module of the Schrödinger software package. Allcompounds were analyzed using Qikprop[4] module of the Small-Molecule Drug Discovery Suite in Schrödinger. Absorption, Distribution, Metabolism, and Excretion (ADME) properties were predicted using the program QikProp where a total of 44 properties can be predicted.

Homology model of A. nidulans GskA

The modeling process by homology consists generally in four different steps (i) template selection; (ii) target template alignment; (iii) model building; and (iv) evaluation. This process can be iteratively repeated, until a satisfying model structure is achieved.

In order to perform the most accurate model, we have selected three pdb structures retrieved from the PDB, 1I09 [23], 1Q5K [24] and 4E7W [21], the first two are human GSK-3β and the last one is *Ustilago maydis* GskA. The sequential alignment was performed using the sequence alignment program CLUSTALX [31]. After templates were selected for model building, the target/template alignment were used as input in the SWISS-MODEL workspace [32, 33] for generating an all-atom model for the target sequence using ProMod-II [34]; by default, models are built using homo-oligomeric structure of the template. An indispensable part of every modelling procedure is the estimation of a protein's model accuracy; here, model quality is assessed with the local

composite scoring function QMEAN (Qualitative Model Energy Analysis), which uses several statistical descriptors expressed as potential of mean force describing the major geometrical aspects of protein structures such as pair wise atomic distances, torsion angles or solvent accessibility. The weights of QMEAN have been specifically retrained for SWISS-MODEL, leading to more accurate local quality predictions.

After building these three models and obtaining pdb structures, we have performed energetic and geometric analysis of all the protein models generated. ProSA [35] is a tool widely used to check 3D models of protein structures for potential errors; its range of application includes error recognition in experimental determined structures, theoretical models and protein engineering. By using this method it has been able to obtain the Z-score value of our models, which is defined as the energy separation between the native fold and the average of an ensemble of misfolds in the units of the standard deviation of the ensemble.

In order to evaluate geometrically quality of the models, PROCHECK [36] has been used. The Ramachandran plot shows the phi-psi torsion angles for all the residues in the structures, being one of the best guides to stereochemical quality. Additionally the models have been evaluated using Verify3D [26, 37], this web server tests energetically the accuracy of the 3D protein model. Finally, the value of RMS (root mean square) has been calculated for the three models.

Fpocket study

In order to determine different cavities on the model of *GskA* enzyme built using homology modelling, the Fpocket software, a highly scalable and free open source pocket detection package, was used. Fpocket [27] is freely available for download at http://www.sourceforge.net/projects/fpocket

Fpocket is an open source pocket detection package based on Voronoi tessellation and alpha spheres built, Voronoi tessellation is performed using the qhull package and more precisely the program qvorono. The Fpocket program could be summarized with three major steps. During the first step the whole ensemble of alpha spheres is determined from the protein structure. Fpocket returns a pre-filtered collection of spheres. The second step consists in identifying clusters of spheres close together, to identify pockets, and to remove

clusters of poor interest. The final step calculates properties from the atoms of the pocket, in order to score each pocket.

As input Fpocket software uses simple standard pdb file, in this case, this file was obtained from our *A. nidulans* GskA protein model. This input file does not contain water molecules, ligands or metal ions. After the structure was studied, the pockets of the protein were organized in a table taking into account the scores giving by the Fpocket program. Then, we have compared the different pocket distribution in the protein and the difference in residues with the template, human GSK-3β (1Q5K), for every binding pocket.

Docking

Before docking calculations, the resulting structure of the homology model was minimized using the option minimize implemented in Sybyl-X 2.1 [38] program. MMFF94 charges and MMFF94 force field [39] were selected, until a 0.01 kcal/mol of gradient was reached, the non-bonding (NB) cutoff used was 10.0 and the dielectric constant 4.0. A distance-dependent dielectric constant was used in all the calculations

All the compounds were set up with Sybyl 2.1 and finally minimized with MMFF94 [39] force field until 0.01 kcal/mol gradient was reached.

Automated docking was used to assess the appropriate binding modes and to explain the different biological behaviour of the tested compounds . A two step protocol was followed; first, a blind docking was carried out for Tideglusib (as covalent reference compound) and VP2.51 (as non-covalent reference compound) in order to know whether the binding site was maintained comparing with the human GSK-3β. Then, a more detailed docking study was performed in the binding site. A Lamarkian genetic algorithm [40] method implemented in the program AutoDock 4.2 [41] was employed; AutoDock suite was used as molecular docking tool in order to carry out the docking simulations. For docking calculations, Gasteiger charges were added, the rotatable bonds were set by AutoDock tools (ADT) and all torsions were allowed to rotate for the ligand. The protein was treated as a rigid molecule, while the ligand as all torsions were treated as flexible. Polar hydrogen atoms were added and Gasteiger charges were assigned to the protein using ADT and AD4 atom type was assigned. The

modified structures obtained were converted in PDBQT format in ADT for AutoDock calculations.

The grid maps were generated by Autogrid program. Each grid was centered at the active pocket of the model protein GskA, and grid parameters were specified separately. To performe blind docking the grid box size was 100x100x100 $Å^3$ points meanwhile in the case of focused docking the grid box size was 40x40x40 $Å^3$ points with a grid-point spacing of 0.375 Å. The docking protocol for consisted of 100 independent Genetic Algorithm (GA) runs per ligand, population size of 150, maximum number of evaluation 2500000, maximum number of 27000 generation, mutation rate of 0.02 and a crossover rate of 0.8 were used for this study. The docking results for a given macromolecule-ligand pair mainly comprised of the intermolecular interaction energies including inhibition constant, hydrogen bond interaction energy, van der Waals forces, electrostatic energy and ligand efficiency. Final best docked clusters (within the default 2.0 Å RMSD) according to the binding energies and relative population provided by Autodock were analyzed by visual inspection.

We have also performed a covalent docking approach according to experimental data for TDZD-8 [22], in this case the grid-based approach calculates a special map for the site of attachment of the covalent ligand. A Gaussian function is constructed with zero energy at the site of attachment and steep energetic penalties at surrounding areas. Docking analysis was performed using a special atom type for the atom that forms the covalent linkage. Analysis of the receptor-ligand complex models was based on energetic score, population of the conformations in the different clusters and interactions. Interactions taken into account were hydrogen bonds, aromatic and hydrophobic ones, all were predicted with the LPC program [42].

Acknowledgments

SAF2012-37979-C03-01to A.M; BFU2012-33142 to E.A.E

Supplementary data

Supplementary data related to this article can be found at …..

References

[1] J.C. Frisvad. Taxonomy, chemodiversity, and chemoconsistency of Aspergillus, Penicillium, and Talaromyces species. Front. Microbiol., 5 (2015) 773.
[2] A. Margalit, K. Kavanagh. The innate immune response to Aspergillus fumigatus at the alveolar surface. FEMS Microbiol. Rev., (2015).
[3] V. Valiante, J. Macheleidt, M. Foge, A.A. Brakhage. The Aspergillus fumigatus cell wall integrity signaling pathway: drug target, compensatory pathways, and virulence. Front Microbiol., 6 (2015) 325.
[4] M. Karthaus, D. Buchheidt. Invasive aspergillosis: new insights into disease, diagnostic and treatment. Curr. Pharm. Des., 19 (2013) 3569-3594.
[5] M. Arvanitis, E. Mylonakis. Diagnosis of invasive aspergillosis: recent developments and ongoing challenges. Eur. J. Clin. Invest., 45 (2015) 646-652.
[6] J. Yaegashi, B.R. Oakley, C.C. Wang. Recent advances in genome mining of secondary metabolite biosynthetic gene clusters and the development of heterologous expression systems in Aspergillus nidulans. J. Ind. Microbiol. Biotechnol., 41 (2015) 433-442.
[7] C. Paulussen, G.A. Boulet, P. Cos, P. Delputte, L.J. Maes. Animal models of invasive aspergillosis for drug discovery. Drug Discov. Today, 19 (2014) 1380-1386.
[8] J. Tilburn, S. Sarkar, D.A. Widdick, E.A. Espeso, M. Orejas, J. Mungroo, M.A. Penalva, H.N. Arst, Jr. The Aspergillus PacC zinc finger transcription factor mediates regulation of both acid- and alkaline-expressed genes by ambient pH. EMBO J., 14 (1995) 779-790.
[9] A. Spielvogel, H. Findon, H.N. Arst, L. Araujo-Bazan, P. Hernandez-Ortiz, U. Stahl, V. Meyer, E.A. Espeso. Two zinc finger transcription factors, CrzA and SltA, are involved in cation homoeostasis and detoxification in Aspergillus nidulans. Biochem. J., 414 (2008) 419-429.
[10] L. Mellado, A.M. Calcagno-Pizarelli, R.A. Lockington, M.S. Cortese, J.M. Kelly, H.N. Arst, Jr., E.A. Espeso. A second component of the SltA-dependent cation tolerance pathway in Aspergillus nidulans. Fungal Genet. Biol., 82 (2015) 116-128.
[11] M.S. Cyert. Calcineurin signaling in Saccharomyces cerevisiae: how yeast go crazy in response to stress. Biochem. Biophys. Res. Commun., 311 (2003) 1143-1150.

[12] P. Hernandez-Ortiz, E.A. Espeso. Phospho-regulation and nucleocytoplasmic trafficking of CrzA in response to calcium and alkaline-pH stress in Aspergillus nidulans. Mol. Microbiol., 89 (2013) 532-551.
[13] G.R. Crabtree, E.N. Olson. NFAT signaling: choreographing the social lives of cells. Cell, 109 Suppl (2002) S67-79.
[14] K. Spinnler, M. Mezger, M. Steffens, H. Sennefelder, O. Kurzai, H. Einsele, J. Loeffler. Role of glycogen synthase kinase 3 (GSK-3) in innate immune response of human immature dendritic cells to Aspergillus fumigatus. Med. Mycol., 48 (2010) 589-597.
[15] C.P. De Souza, S.B. Hashmi, A.H. Osmani, P. Andrews, C.S. Ringelberg, J.C. Dunlap, S.A. Osmani. Functional analysis of the Aspergillus nidulans kinome. PLoS One, 8 (2013) e58008.
[16] J.E. Galagan, S.E. Calvo, C. Cuomo, L.J. Ma, J.R. Wortman, S. Batzoglou, S.I. Lee, M. Basturkmen, C.C. Spevak, J. Clutterbuck, V. Kapitonov, J. Jurka, C. Scazzocchio, M. Farman, J. Butler, S. Purcell, S. Harris, G.H. Braus, O. Draht, S. Busch, C. D'Enfert, C. Bouchier, G.H. Goldman, D. Bell-Pedersen, S. Griffiths-Jones, J.H. Doonan, J. Yu, K. Vienken, A. Pain, M. Freitag, E.U. Selker, D.B. Archer, M.A. Penalva, B.R. Oakley, M. Momany, T. Tanaka, T. Kumagai, K. Asai, M. Machida, W.C. Nierman, D.W. Denning, M. Caddick, M. Hynes, M. Paoletti, R. Fischer, B. Miller, P. Dyer, M.S. Sachs, S.A. Osmani, B.W. Birren. Sequencing of Aspergillus nidulans and comparative analysis with A. fumigatus and A. oryzae. Nature, 438 (2005) 1105-1115.
[17] V. Palomo, I. Soteras, D.I. Perez, C. Perez, C. Gil, N.E. Campillo, A. Martinez. Exploring the binding sites of glycogen synthase kinase 3. Identification and characterization of allosteric modulation cavities. J. Med. Chem., 54 (2011) 8461-8470.
[18] S. Conde, D.I. Perez, A. Martinez, C. Perez, F.J. Moreno. Thienyl and phenyl alpha-halomethyl ketones: new inhibitors of glycogen synthase kinase (GSK-3beta) from a library of compound searching. J. Med. Chem., 46 (2003) 4631-4633.
[19] V. Palomo, D.I. Perez, C. Perez, J.A. Morales-Garcia, I. Soteras, S. Alonso-Gil, A. Encinas, A. Castro, N.E. Campillo, A. Perez-Castillo, C. Gil, A. Martinez. 5-imino-1,2,4-thiadiazoles: first small molecules as substrate competitive inhibitors of glycogen synthase kinase 3. J. Med. Chem., 55 (2012) 1645-1661.

[20] A. Martinez, M. Alonso, A. Castro, C. Perez, F.J. Moreno. First non-ATP competitive glycogen synthase kinase 3 beta (GSK-3beta) inhibitors: thiadiazolidinones (TDZD) as potential drugs for the treatment of Alzheimer's disease. J. Med. Chem., 45 (2002) 1292-1299.
[21] C. Grutter, J.R. Simard, S.C. Mayer-Wrangowski, P.H. Schreier, J. Perez-Martin, A. Richters, M. Getlik, O. Gutbrod, C.A. Braun, M.E. Beck, D. Rauh. Targeting GSK3 from Ustilago maydis: type-II kinase inhibitors as potential antifungals. ACS Chem. Biol., 7 (2012) 1257-1267.
[22] J.M. Dominguez, A. Fuertes, L. Orozco, M. del Monte-Millan, E. Delgado, M. Medina. Evidence for irreversible inhibition of glycogen synthase kinase-3beta by tideglusib. J. Biol. Chem., 287 (2012) 893-904.
[23] E. ter Haar, J.T. Coll, D.A. Austen, H.M. Hsiao, L. Swenson, J. Jain. Structure of GSK3beta reveals a primed phosphorylation mechanism. Nat. Struct. Biol., 8 (2001) 593-596.
[24] R. Bhat, Y. Xue, S. Berg, S. Hellberg, M. Ormo, Y. Nilsson, A.C. Radesater, E. Jerning, P.O. Markgren, T. Borgegard, M. Nylof, A. Gimenez-Cassina, F. Hernandez, J.J. Lucas, J. Diaz-Nido, J. Avila. Structural insights and biological effects of glycogen synthase kinase 3-specific inhibitor AR-A014418. J. Biol. Chem, 278 (2003) 45937-45945.
[25] P. Benkert, S.C. Tosatto, D. Schomburg. QMEAN: A comprehensive scoring function for model quality assessment. Proteins, 71 (2008) 261-277.
[26] D. Eisenberg, R. Luthy, J.U. Bowie. VERIFY3D: assessment of protein models with three-dimensional profiles. Methods Enzymol., 277 (1997) 396-404.
[27] V. Le Guilloux, P. Schmidtke, P. Tuffery. Fpocket: an open source platform for ligand pocket detection. BMC bioinformatics, 10 (2009) 168.
[28] A. Markina-Inarrairaegui, O. Etxebeste, E. Herrero-Garcia, L. Araujo-Bazan, J. Fernandez-Martinez, J.A. Flores, S.A. Osmani, E.A. Espeso. Nuclear transporters in a multinucleated organism: functional and localization analyses in Aspergillus nidulans. Mol. Biol. Cell, 22 (2011) 3874-3886.
[29] J. Tilburn, C. Scazzocchio, G.G. Taylor, J.H. Zabicky-Zissman, R.A. Lockington, R.W. Davies. Transformation by integration in Aspergillus nidulans. Gene, 26 (1983) 205-221.

[30] T. Nayak, E. Szewczyk, C.E. Oakley, A. Osmani, L. Ukil, S.L. Murray, M.J. Hynes, S.A. Osmani, B.R. Oakley. A versatile and efficient gene-targeting system for Aspergillus nidulans. Genetics, 172 (2006) 1557-1566.

[31] M.A. Larkin, G. Blackshields, N.P. Brown, R. Chenna, P.A. McGettigan, H. McWilliam, F. Valentin, I.M. Wallace, A. Wilm, R. Lopez, J.D. Thompson, T.J. Gibson, D.G. Higgins. Clustal W and Clustal X version 2.0. Bioinformatics, 23 (2007) 2947-2948.

[32] K. Arnold, L. Bordoli, J. Kopp, T. Schwede. The SWISS-MODEL workspace: a web-based environment for protein structure homology modelling. Bioinformatics, 22 (2006) 195-201.

[33] T. Schwede, J. Kopp, N. Guex, M.C. Peitsch. SWISS-MODEL: An automated protein homology-modeling server. Nucleic acids research, 31 (2003) 3381-3385.

[34] N. Guex, M.C. Peitsch. SWISS-MODEL and the Swiss-PdbViewer: an environment for comparative protein modeling. Electrophoresis, 18 (1997) 2714-2723.

[35] M. Wiederstein, M.J. Sippl. ProSA-web: interactive web service for the recognition of errors in three-dimensional structures of proteins. Nucleic acids research, 35 (2007) W407-410.

[36] R.A. Laskowski, D.S. Moss, J.M. Thornton. Main-chain bond lengths and bond angles in protein structures. J. Mol. Biol., 231 (1993) 1049-1067.

[37] R. Luthy, J.U. Bowie, D. Eisenberg. Assessment of protein models with three-dimensional profiles. Nature, 356 (1992) 83-85.

[38] Sybyl-X 2.1, Tripos International, 1699 South Hanley Rd., St Louis, Missouri, 63144, USA.

[39] P.A. Halgren, Merck Merck molecular force field. II. MMFF94 van der Waals and electrostatic parameters for intermolecular interactions. J. Comput. Chem, 17 (1996) 520-552.

[40] D.S.G. Garrett M. Morris, Robert S. Halliday, Ruth Huey, William E. Hart, Richard K. Belew andArthur J. Olson. Automated docking using a Lamarckian genetic algorithm and an empirical binding free energy function. J. Comput. Chem., 19 (1998) 1639–1662.

[41] G.M. Morris, R. Huey, W. Lindstrom, M.F. Sanner, R.K. Belew, D.S. Goodsell, A.J. Olson. AutoDock4 and AutoDockTools4: Automated docking with selective receptor flexibility. J. Comput. Chem., 30 (2009) 2785-2791.
[42] V. Sobolev, A. Sorokine, J. Prilusky, E.E. Abola, M. Edelman. Automated analysis of interatomic contacts in proteins. Bioinformatics, 15 (1999) 327-332.